Available online at www.sciencedirect.com
SCIENCE DIRECT®
Journal of Sound and Vibration 268 (2003) 971–991
JOURNAL OF SOUND AND VIBRATION
www.elsevier.com/locate/jsvi

Maximum likelihood identification of non-stationary operational data

E. Parloo*, P. Guillaume, B. Cauberghe

Department of Mechanical Engineering, Vrije Universiteit Brussel, Pleinlaan 2, B-1050 Brussels, Belgium

Received 29 July 2002; accepted 28 November 2002

Abstract

In-operation modal analysis has become a valid alternative for structures where a classic input–output test would be difficult if not impossible to conduct. Due to practical considerations, measurements are sometimes performed in patches (roving sensor setups) instead of covering the entire structure at once. In practice, one is often confronted with non-stationary ambient excitation sources (e.g., wind, traffic, waves, etc.). Since the scaling of operational mode shape estimates depends on the unknown level of the ambient excitation, an extra effort is required in order to correctly merge the different parts of the mode shapes. In this contribution, two different approaches, for merging operational mode shapes from non-stationary data, are proposed. Both methods are based upon a single maximum likelihood estimation procedure. For comparison and validation, both techniques were applied to non-stationary data sets obtained by scanning laser vibrometry as well as the Z24 bridge bench mark data.

1. Introduction

For a great deal of mechanical structures, the determination of modal models from classic input–output forced vibration tests may prove to be a difficult, if not impossible, task at least with standard testing material. For instance, civil structures (e.g., bridges, buildings, off-shore platforms, etc.) and machinery, in operating conditions, are excited by unmeasurable ambient excitation sources (e.g., traffic, wind, waves, etc.). If an artificial excitation device is used, the presence of all other non-measured forces that act upon the structure (ambient excitation) will lead to a deterioration of the quality of the classic input–output model derived from the data. Industrial-economical considerations often prevent a complete shutdown of the device under test (e.g., closing bridge to traffic, shutting down production lines, etc.) to improve conditions for

*Corresponding author. Tel.: +32-2-629-2807; fax: +32-2-629-2865.
E-mail address: eli.parloo@vub.ac.be (E. Parloo).

0022-460X/03/$ - see front matter © 2003 Elsevier Ltd. All rights reserved.
doi:10.1016/S0022-460X(03)00377-8

classic forced vibration modal testing. Since in-operation analysis deals with output-only data, all excitation forces (including those which are hard or impossible to measure) are taken into account. Moreover, the use of appropriate artificial excitation devices (large shakers, drop weights) can be considered as both expensive and impractical [1,2]. On the other hand, the use of ambient excitation sources is cheap and freely available.

The expansion of model-based system identification techniques, such as maximum likelihood (ML) estimators [3], subspace-based techniques [2,4] etc., to the domain of output-only data, has allowed the identification of modal models from in-operation structures. The modelling of output-only data, obtained from naturally excited structures, is particularly interesting because the test structure remains in its normal in-operation condition during the test. This can be considered as an advantage, since the condition of the test structure during a laboratory forced-vibration test often differs significantly from the structure's real in-operation working conditions. An example is given by high-speed ships where the mass loading of water adjacent to the hull varies with the speed of the ship through the water [5]. Since changes in mass-loading induce changes in modal parameters, the dynamic behavior of the ship will depend upon its speed. Other vehicles or structures (e.g., bridges open for traffic, offshore platforms, cars, trains, …) show a similar behavior to changes in working condition [6–10]. One of the drawbacks of operational analysis is that part of the modal parameters can no longer be estimated. Since the ambient forces that excite the test structure are not being measured, the estimated operational mode shapes remain incorrectly scaled with scaling factors dependant on the unknown ambient excitation [11]. This means that, when dealing with non-stationary signals, the scaling of the mode shapes will be different from test to test.

In practice, when confronted with large structures or when a high spatial resolution is required, measurements cannot always be performed in all degrees of freedom (d.o.f.'s) at once. A number of subsequent measurements, performed in different setups (patches), is then required to cover all intended d.o.f.'s of the structure [1]. Since ambient excitation sources often have a non-stationary nature (e.g., wind, traffic, waves, etc.), an extra effort is needed to correctly reassemble (re-scale) the different parts of the mode shapes obtained from output-only data. For this reason, one or more reference responses are to be measured simultaneously with each of the different setups (patches). A separate identification procedure, for all considered patches and their references, can be used in order to correctly reassemble the mode shapes. If a large number of patches are used, this procedure becomes a lengthy and tiresome operation. Moreover, the use of such technique yields more than one set of natural frequency and damping ratio estimates. Making an objective choice among these sets often proves to be difficult [12–14]. In Ref. [15], the idea was explored to re-scale and merge the data from the different patches before performing the system identification step. For this purpose, the subspace-based output-only identification technique was adapted to handle multi-patch measurement setups.

In this contribution, two different method are presented for the extraction of correctly assembled mode shape estimates from an estimation procedure applied to the complete set of data gathered by all patches. Throughout this paper, a frequency-domain maximum likelihood (ML) identification technique was used for the modal parameter estimation. It should be noted that the presented techniques are not restricted to ML identification. A comparison is made between a non-parametric and a parametric approach, where the unwanted non-stationary effects are removed respectively before and after the system identification step. For comparison and

validation purpose, results were used from experiments performed on a clamped plate as well as from the Z24 bridge bench mark data.

2. Theoretical aspects

Some of the theoretical aspects related to the presented work will be briefly discussed in the following sections.

2.1. Modal decomposition of power spectra

Consider an n d.o.f. representation of a linear mechanical system. Let $\{\mathbf{f}(t)\}$ denote the $(n \times 1)$ force input vector at continuous time t and $\{\mathbf{x}(t)\}$ the $(n \times 1)$ output displacement vector. Let the $(n \times n)$ frequency response function (FRF) matrix between the outputs and inputs be given by

$$[\mathbf{H}(\omega)] = \begin{bmatrix} H_{11}(\omega) & \cdots & H_{n1}(\omega) \\ \vdots & \ddots & \vdots \\ H_{1n}(\omega) & \cdots & H_{nn}(\omega) \end{bmatrix}. \tag{1}$$

According to the modal theory of mechanical systems, the FRF matrix can be decomposed as follows

$$[\mathbf{H}(\omega)] = \sum_{s=1}^{N_m} \left(\frac{\{\boldsymbol{\phi}_s\}\{\mathbf{L}_s\}^{\mathrm{T}}}{(\mathrm{j}\omega - \lambda_s)} + \frac{\{\boldsymbol{\phi}_s\}^*\{\mathbf{L}_s\}^{\mathrm{H}}}{(\mathrm{j}\omega - \lambda_s^*)} \right), \tag{2}$$

where λ_s, $\{\boldsymbol{\phi}_s\}$ and $\{\mathbf{L}_s\}$ are, respectively, the pole, mode shape and modal participation factor of mode s, with N_m the number of modes. The mathematical operators transpose, complex conjugate and hermitian conjugate are respectively denoted as $[\cdot]^{\mathrm{T}}$, $[\cdot]^*$ and $[\cdot]^{\mathrm{H}}$.

Since the force signals are not measured during an in-operation analysis (output-only data), FRFs can no longer be estimated and used for system identification purposes. The approach we will follow here consists in replacing the FRFs by cross power spectra of the outputs, a quantity that can be derived from output-only measurements. For stationary stochastic processes $\{\mathbf{f}(t)\}$, the $(n \times n)$ cross power matrix of the outputs, $[\mathbf{S_{XX}}(\omega)]$, is given by

$$[\mathbf{S_{XX}}(\omega)] = [\mathbf{H}(\omega)][\mathbf{S_{FF}}(\omega)][\mathbf{H}(\omega)]^{\mathrm{H}}, \tag{3}$$

where $[\mathbf{S_{FF}}(\omega)]$ is the cross power matrix of the (unknown) input forces. By substituting Eq. (2) in Eq. (3) and assuming white-noise inputs, it is easily shown that the cross power matrix of the outputs can be modally decomposed as follows

$$\begin{aligned}[\mathbf{S_{XX}}(\omega)] = & \sum_{s=1}^{N_m} \left(\frac{\{\boldsymbol{\psi}_s\}\{\mathbf{Q}_s\}^{\mathrm{T}}}{(\mathrm{j}\omega - \lambda_s)} + \frac{\{\boldsymbol{\psi}_s\}^*\{\mathbf{Q}_s\}^{\mathrm{H}}}{(\mathrm{j}\omega - \lambda_s^*)} \right) \\ & + \sum_{s=1}^{N_m} \left(\frac{\{\mathbf{Q}_s\}\{\boldsymbol{\psi}_s\}^{\mathrm{T}}}{(-\mathrm{j}\omega - \lambda_s)} + \frac{\{\mathbf{Q}_s\}^*\{\boldsymbol{\psi}_s\}^{\mathrm{H}}}{(\mathrm{j}\omega - \lambda_s^*)} \right), \end{aligned} \tag{4}$$

where $\{\boldsymbol{\psi}_s\}$ and $\{\mathbf{Q}_s\}$ are, respectively, the operational mode shape and reference vector for mode s. This reference vector is a complex function of the cross power matrix of the unknown random

input force(s) and the modal parameters of the structure. Since the modal participation factors can no longer be determined, the operational mode shapes $\{\psi_s\}$ remain unscaled dependant on the unknown operational forces acting on the structure.

Eq. (4) forms the basis for frequency-domain output-only modal analysis. It shows that by using cross power estimates, between the responses and a number of reference responses, modal models can be obtained from structures in their operating condition. On a basis of the measured response sequences, several techniques can be used to obtain estimates of the auto and cross power spectra [16,17]. A well-known and often used method is the so-called periodogram approach [16,18].

It should be noted that a white spectrum noise excitation signal is assumed in the in-operation modal analysis theory. If the structure is excited by colored ambient noise, additional peaks can appear into the spectra that are not related to resonances of the system (e.g., presence of engine rotation speed harmonics, etc.). If this is the case, these extra peaks should be distinguished from the real structural resonances. In most cases, some pre-knowledge about the working conditions of the in-operation structure is sufficient to discriminate the colored excitation poles from true physical modes. An overview of other possible techniques and their application is given in Ref. [19].

2.2. Maximum likelihood identification

In Ref. [20] a frequency-domain ML estimator was proposed for the identification of modal parameters from input-output FRF measurements. It was shown in Ref. [3] that a similar approach can be used for the estimation of modal parameters from cross power functions of response measurements. Like FRFs, the cross power spectra of the outputs can be modelled by means of a common-denominator transfer function model

$$\hat{H}_{or}(\omega_f) = \frac{N_{or}(\omega_f)}{D(\omega_f)}, \tag{5}$$

for $r = 1, \ldots, N_{ref}$ and $o = 1, \ldots, N_o$ with

$$N_{or}(\omega_f) = \sum_{k=o}^{n} \Omega_k(\omega_f) B_{ork} \tag{6}$$

the numerator polynomial between output o and input (reference-response) r

$$D(\omega_f) = \sum_{k=o}^{n} \Omega_k(\omega_f) A_k, \tag{7}$$

the common denominator polynomial. The polynomial basis functions $\Omega_k(\omega_f)$ are given by $\Omega_k(\omega_f) = \mathrm{e}^{-\mathrm{j}\omega_f T_s k}$ (i.e., a discrete-time model with T_s the sampling period is used). The coefficients A_k and B_{ork} are the parameters to be estimated. They will be represented by θ in the sequel of this section.

Assuming the measured power spectra, $S_{or}(\omega_f)$ between output o and reference-response r, to be (complex) normally distributed and mutually uncorrelated, the (negative) log-likelihood function

reduces to [20,21]

$$\ell_{ML}(\theta) = \sum_{o=1}^{N_o} \sum_{r=1}^{N_{ref}} \sum_{f=1}^{N_f} \frac{|\hat{H}_{or}(\theta, \omega_f) - S_{or}(\omega_f)|^2}{\mathrm{var}\{S_{or}(\omega_f)\}}. \tag{8}$$

The ML-estimate of θ (i.e., the polynomial coefficients) is obtained by minimizing Eq. (8). This can be done by means of a Gauss–Newton optimization algorithm which takes advantage of the quadratic form of the cost function (8). During the ML-estimation process, uncertainty information, $\mathrm{var}\{S_{or}(\omega_f)\}$, is taken into account. This way, more weight is set upon measurements with a high signal-to-noise ratio (low uncertainty) than on measurements with a low signal-to-noise ratio (high uncertainty). Taking noise information into account usually leads to more accurate estimation results [3,20]. The uncertainty on the measurements can be derived by means of several approaches depending on the nature of the data (input–output or output-only [3,20], stationary or non-stationary signals [22], …). In this contribution, a method based upon the residual errors from a preliminary least-squares estimation was employed for both output-only and input-output data sets [22].

2.3. Assembly of mode shapes from different patches

2.3.1. Introduction

In practice, when confronted with large structures or a high spatial resolution is required, measurements cannot always be performed in all d.o.f.'s at once. In order to cover all intended d.o.f.'s of the structure, subsequent measurements performed in different setups (patches) are required. A first example is given by modal testing on civil structures [1,2]. Due to the high cost of the measurement equipment, a limited amount of sensors (accelerometers) is usually employed. Another example is given by scanning laser vibrometry (SLV). In this case, the laser beam can only scan one point at the time resulting in a large number of measurement patches. If the force(s) that excite the structure are being simultaneously measured, no additional efforts are required to correctly assemble the mode shape estimates from the different patches. By measuring the force(s), scaled quantities such as FRFs can be obtained.

During an in-operation modal analysis, only part of the modal model can be determined. Since the ambient forces that excite the structure are not measured, the modal participation factors cannot be determined. As a result, the estimated mode shape vectors remain unscaled, i.e., dependant on the unknown level of excitation [11]. If the excitation is of a non-stationary nature, the scaling of the estimated mode shapes will be different from test to test. Since ambient excitation sources often have a non-stationary nature (e.g., wind, traffic, waves, etc.), an extra effort is needed to correctly reassemble (re-scale) the mode shapes obtained from the different patches of output-only data [15]. For this reason, one or more reference responses are to be measured simultaneously with each of the different setups (patches) [1].

Different sorts of non-stationarity can be distinguished.

A first type to be considered is excitation level instability, where the level of excitation becomes a function of time. In this case, re-scaling methods that are simply based on the computation of spectral RMS values [23] might be sufficient to compensate the non-stationarity in the spectral estimates.

A second type of non-stationarity to consider is the so-called excitation color or mode participation instability. In this case, the excitation levels for some particular modes or frequency ranges can be instable. Compensation for this type of instability (possibly combined with excitation level instability) requires more advanced methods based on the measurement of reference responses in one or more d.o.f.'s common to all considered patches (Sections 2.3.2–2.3.4).

Performing vibration measurements on a structure, by means of roving patches, also increases the possibility on data non-stationarity that is independent of the excitation. For instance, the mass loading effect of a set of roving accelerometers can cause changes in the modal parameters of the structure. Even if the mass loading effect of roving sensors is negligible (e.g., civil engineering structures) or SLV is used for response measurement, changes in environmental conditions (e.g., temperature, moisture) can still lead to similar changes. Since this type of non-stationarity depends on the variability of the structure with respect to time, it is often referred to as data inconsistency [12,13].

The methods, presented in the following sections, were designed to compensate for both excitation level and modal participation non-stationarity. However, all discussed methods assume that the modal properties of the structure are independent of the measurement patch (i.e., possible data inconsistency is not considered).

Furthermore, although a ML estimator was used is this paper for the system identification process, it should be pointed out that the described assembly techniques are not limited to this specific system identification algorithm.

2.3.2. Classic assembly approach

A separate identification procedure, for all N_P considered patches including their N_{ref} corresponding reference responses, can be used in order to correctly assemble the mode shape estimates (Fig. 1). Each system identification procedure involves the estimation of the modal parameters from each patch and the discrimination between the true physical modes and the so-called mathematical or spurious modes. After N_P system identification processes, the mode shapes can be 'glued' to one another by using the mode shape estimation results from the reference d.o.f.'s common in the different patches.

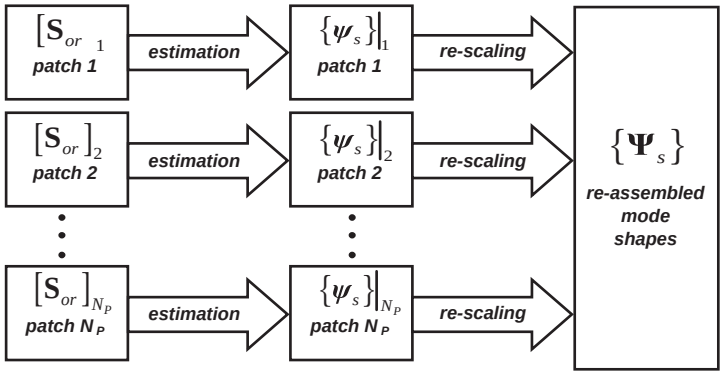

Fig. 1. Flow chart of lengthy re-scaling procedure.

Before this is possible, an additional mode pairing procedure is required between the identification results obtained from the different patches. A disadvantage, or even problem, to the need of such a procedure is that, for some patches, the possibility exists that not all modes are clearly observable/identifiable in the data. This can be the case if, for instance, all sensors of a given patch are located in or near nodal points for a certain mode of interest. On the other hand, the use of separate identification procedures in combination with mode pairing could be considered an advantage if data inconsistencies are present between the different patches.

If a large number of patches are used (e.g., high spatial resolution with SLV-experiments, etc.), the classic assembly procedure becomes a lengthy and tiresome operation. Even with the help of autonomous system identification procedures [24], for discriminating the true physical modes among the mathematical ones, preference should still be given to a global estimation approach while assuming the absence of data inconsistency. Moreover, the use of a separate system identification procedure for each patch yields more than one set of natural frequency and damping ratio estimates which makes it difficult to make an objective decision [12–14].

2.3.3. *Parametric assembly approach*

Instead of performing a separate estimation for every patch, a single estimation procedure can be performed on the complete set of data obtained from all patches together with their reference responses (Fig. 2). Apart from the normal N_o outputs measured in the intended experimental d.o.f.'s of the test structure, an additional amount of $(N_{ref} \times N_P)$ reference d.o.f.'s will be present. After the estimation procedure, yielding a single set of natural frequency and damping ratio estimates, the different patches of the mode shapes can still be correctly assembled by making use of the estimates found for the references common to all patches. If the same reference d.o.f.'s were measured in all considered patches, the following expressions can be used for re-scaling the mode shape vectors $\{\boldsymbol{\phi}_s\}|_j$ of patch j $(j = 1, \ldots, N_P)$ and mode s $(s = 1, \ldots, N_m)$, to a common level as for instance dictated by patch $k \in \{1, \ldots, N_P\}$.

$$\{\boldsymbol{\phi}_s\}|_{j \to k} = \alpha_{js} \cdot \{\boldsymbol{\phi}_s\}|_j, \tag{9}$$

with

$$\alpha_{js} = \frac{\{\boldsymbol{\phi}_s^{ref}\}^{\mathrm{T}}|_j \{\boldsymbol{\phi}_s^{ref}\}|_k}{\{\boldsymbol{\phi}_s^{ref}\}^{\mathrm{T}}|_j \{\boldsymbol{\phi}_s^{ref}\}|_j}, \tag{10}$$

and $\{\boldsymbol{\phi}_s^{ref}\}|_j$ the mode shape vector of mode s with the reference responses of patch j. It should be noted that in expression (10), α_{js} is computed in the same way as a modal scaling factor [25]. Since

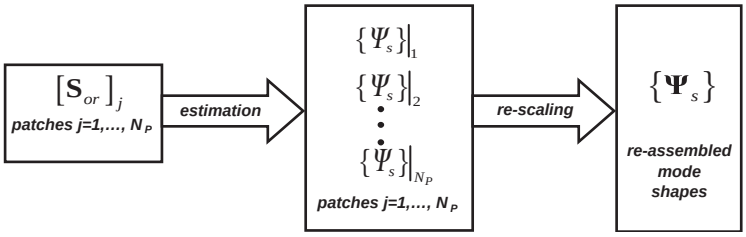

Fig. 2. Flow chart of parametric re-scaling procedure.

the re-scaling takes place after the system identification process, the expression 'parametric' reassembly approach was used to indicate this method in the remainder of the text.

The parametric assembly approach assumes that the different patches all yield information on the same system. A violation of this assumption, due to the presence of data inconsistency, will lead to identification problems due to the fact that all data is processed as one set [12,13]. Although the classic approach would have been less trouble due to the separate estimation procedures and the subsequent mode pairing, the data inconsistency errors would still be present in the mode shape estimates.

The quality of the re-scaling results will greatly depend on the choice of suitable reference responses. Any a priori knowledge of the mode shapes (e.g., from a preliminary finite element model or measurements) can help in making this choice. Locations where signals can be obtained with a high signal-to-noise ratio, should be preferred for the placement of reference sensors. Such positions are usually located in extremes of the mode shapes, away from nodal points of the modes of interest. Although a suitable location for one mode (extreme mode shape value) might be a nodal point for another, at least one good reference response should be obtained for each modes to be considered for identification. Choosing all reference sensors in nodal points of a given mode will decimate the observability/identifiability of that mode in the resulting auto and cross power estimates. Needless to say that this will have a negative effect on the re-scaling results for that mode. The same remarks can be made for the classic assembly approach (Section 2.3.2) and the non-parametric approach described in the following section.

2.3.4. *Non-parametric assembly approach*

As an alternative to the parametric approach, the re-scaling of the different patches can be performed before the system identification step (Fig. 3). This approach will be referred to as the non-parametric method in the remainder of the text. If N_{ref} reference responses are used, the cross power spectra $[\mathbf{S}_{or}(\omega)]|_j$ for all frequencies ω of each patch j ($j = 1, \ldots, N_P$) can be re-scaled to a common level dictated by, for instance, the $(N_{ref} \times N_{ref})$ reference matrix $[\mathbf{S}_{or}^{ref}(\omega)]|_k$ from patch k (with $k \in \{1, \ldots, N_P\}$)

$$[\mathbf{S}_{or}(\omega)]|_{j\to k} = [\mathbf{S}_{or}(\omega)]|_j \cdot ([\mathbf{S}_{or}^{ref}(\omega)]|_j)^{-1} \cdot [\mathbf{S}_{or}^{ref}(\omega)]|_k. \tag{11}$$

A system identification step on this re-scaled data directly yields correctly assembled mode shape vectors $\{\boldsymbol{\Psi}_s\}$ for each mode s in the considered frequency band. By dividing the data from patch j by its reference data, the poles from the system are lost. Transmissibility functions are obtained with peaks that are no longer evidence of system resonances. In order to circumvent this problem, the transmissibilities are multiplied by the same reference patch k. This reference data contains the system poles, which brings the poles back into the re-scaled data. Due to the non-stationary

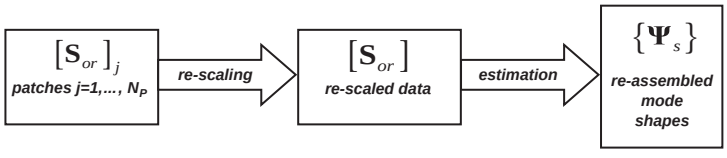

Fig. 3. Flow chart of non-parametric re-scaling procedure.

nature of the ambient excitation, the arbitrary chosen reference patch k can be of poor quality. Instead of choosing a single patch k, an average can be used for each of the references common to all patches:

$$[\mathbf{S}_{or}(\omega)]|_{j\to\Sigma} = [\mathbf{S}_{or}(\omega)]|_j \cdot ([\mathbf{S}_{or}^{ref}(\omega)]|_j)^{-1} \cdot \frac{1}{N_P}\sum_{k=1}^{N_P}[\mathbf{S}_{or}^{ref}(\omega)]|_k. \tag{12}$$

The latter approach will yield a better overall signal-to-noise ratio for the re-scaled data.

Similar to the parametric approach, the non-parametric assembly method assumes the absence of data inconsistency between the different patches. A violation of this assumption will have a negative effect on the re-scaling results since the peaks in Eq. (11) will no longer fully coincide.

3. Experimental results

3.1. Output-only scanning laser vibrometry experiments

A good example of a measurement technique that works with a high number of patches is SLV. Since the laser beam can only measure one point at the time, application of this technique results in a number of patches equal to the number of measurement points. Since SLV is often used for obtaining measurements with a high spatial resolution, a large number of patches is usually obtained. If the force(s) that excite the structure are being simultaneously measured (input–output data) or the ambient excitation (output-only data) can be considered stationary, no additional efforts are required to correctly assemble the mode shape estimates from the different patches. In the case of stationary output-only data, one (or more) well chosen reference responses can be used for obtaining the desired cross power estimates for direct use with the ML estimator. However, if the ambient excitation source is non-stationary, one of the described techniques will be required in order to correctly assemble the mode shape estimates.

It should be noted that if all required time domain sequences (responses and reference responses) are stored (instead of immediate data processing to the frequency domain), SLV of non-stationary output-only data requires the measurement of $(N_{ref}+1)N_o$ data sequences. This is $(N_{ref}+1)$ times more than the case were all outputs would have been measured at once.

As an illustration, the following experiments were conducted. A (300 mm × 280 mm × 4 mm) composite plate was clamped by one side onto a vast concrete slab in laboratory conditions (Fig. 4). Velocity responses were measured subsequently in all 224 points (organized in areas A–E) with a Polytec PSV-300 scanning laser vibrometer. For each measurement, a simultaneous reference response measurement was performed in point 1 of the structure by means of a Polytec OFV-501 single-point laser vibrometer. This way, no physical contact was required with the test structure during the vibration measurements.

A stationary output-only data set was obtained while the structure was acoustically excited (with a speaker at the back of the plate) by means of a periodic chirp signal. All areas were scanned with the same stationary level of excitation. The auto and cross power estimates were obtained from 5 averages and contained 800 spectral lines in a bandwidth up to 1000 Hz. At this point, a single ML estimation on the measured cross power spectra (between the measurements and their reference) is sufficient to directly obtain correctly assembled mode shape estimates. An

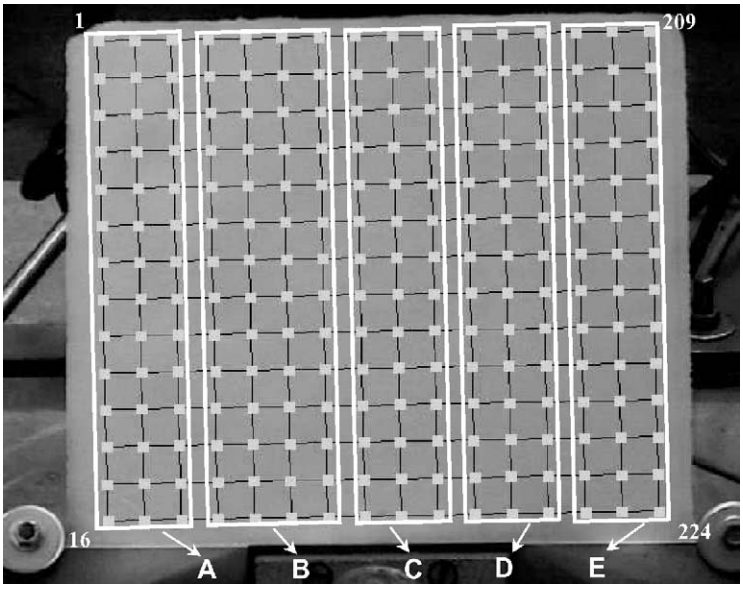

Fig. 4. Composite plate with clamped bottom side. Applied SLV 224 point measurement grid divided into virtual areas A–E.

Table 1
Overview of the estimation results obtained for the clamped plate: acoustic excitation

Stationary		Non-stationary					
No re-scaling		No re-scaling		Parametric		Non-parametric	
ω (Hz)	ξ (%)	ω (Hz)	ξ (%)	ω (Hz)	ξ (%)	ω (Hz)	ξ (%)
15.36	0.21	15.34	2.45	15.74	0.85	15.80	0.73
78.78	0.42	78.83	0.44	78.67	0.58	78.83	0.43
103.99	0.52	104.00	0.53	103.97	0.48	104.02	0.51
106.44	0.41	106.45	0.39	106.75	0.02	106.50	0.49
112.06	0.40	112.03	0.40	112.00	0.41	112.03	0.40

overview of the obtained natural frequency and damping ratio estimates for modes 1–5 is given in Table 1. The mode shape estimates obtained for modes 2 and 3 are shown in Figs. 5(a)–(b).

Next, a non-stationary output-only data set was obtained by scanning the plate with a different level of periodic chirp excitation for each area A–E of measurement points. Due to the non-stationary nature of the data, a global ML estimation on all 224 cross power spectra does no longer yield correctly assembled mode shape estimates. The effect of the different level of excitation used for each area, can clearly be observed in the mode shape estimates (Figs. 5(c)–(d)). The most straightforward approach (often used in civil engineering, schematically depicted in Fig. 1), would involve 224 separate estimation procedures for each of the measurement patches. This method would also yield 224 different sets of natural frequency and damping ratio estimates.

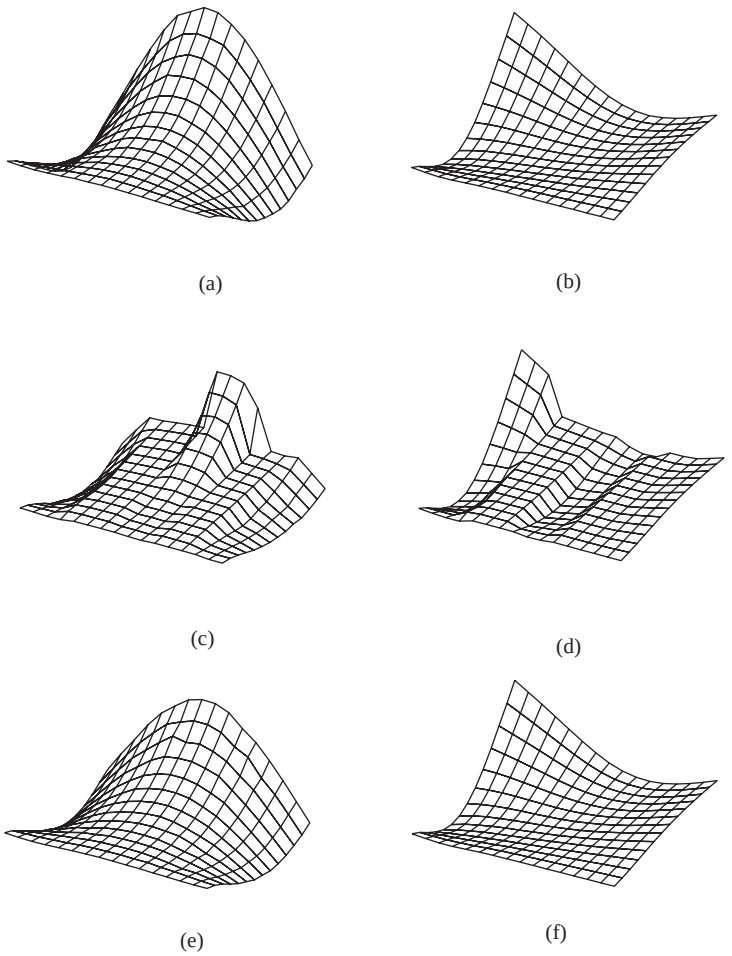

Fig. 5. Mode shape estimates of modes 2 and 3 obtained from plate with acoustic excitation. Stationary excitation without re-scaling: a–b, non-stationary excitation without re-scaling: c–d, non-stationary excitation with re-scaling: e–f.

By using the described parametric (Fig. 2) or non-parametric (Fig. 3) re-scaling approach, correctly assembled mode shape estimates can be obtained from a single ML estimation procedure yielding 1 set of natural frequency and damping ratio estimates. An overview of the natural frequency and damping ratio estimates for both approaches on the non-stationary data can be found in Table 1. The mode shape estimates for modes 2–3 found with the parametric approach are shown in Figs. 5(e)–(f). Similar results were found with the non-parametric approach.

So far, the preceding experiments involved an acoustic excitation of the test structure by means of a periodic chirp signal. By using a controlled excitation technique, a good signal-to-noise ratio can usually be obtained. In practice, one is often confronted with in-operational data with a poor signal-to-noise ratio due to low ambient excitation levels. Moreover, some modes can be better excited than others. These aspects will have their influence on the performance of the described re-scaling techniques. For this reason, an additional data set was measured without the acoustic

Table 2
Overview of the estimation results obtained for the clamped plate: ambient excitation

Mode	No re-scaling		Parametric		Non-parametric	
	ω (Hz)	ξ (%)	ω (Hz)	ξ (%)	ω (Hz)	ξ (%)
1	15.81	0.56	15.85	0.39	15.66	0.63
2	81.46	0.55	81.39	0.50	81.43	0.60
3	104.81	0.52	104.87	0.49	104.84	0.60
4	—	—	105.74	0.86	108.33	0.64
5	112.94	0.54	112.81	0.36	112.95	0.49

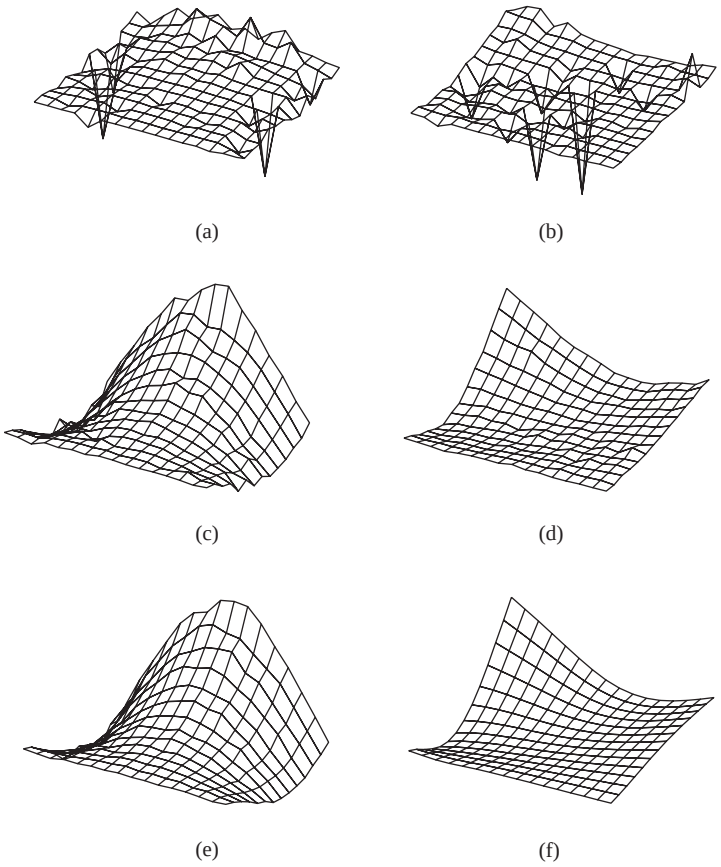

Fig. 6. Mode shape estimates obtained from plate with ambient excitation: modes 2 and 3, without re-scaling a–b, with parametric re-scaling c–d, with non-parametric re-scaling e–f.

excitation device. This time, the plate was excited by non-stationary ambient noise and vibration produced by the traffic in the street nearby our laboratory. All auto and cross power estimates were obtained from 5 averages containing 3200 spectral lines in a bandwidth up to 1000 Hz. Table 2 shows the results for both the parametric and non-parametric re-scaling approach, as well

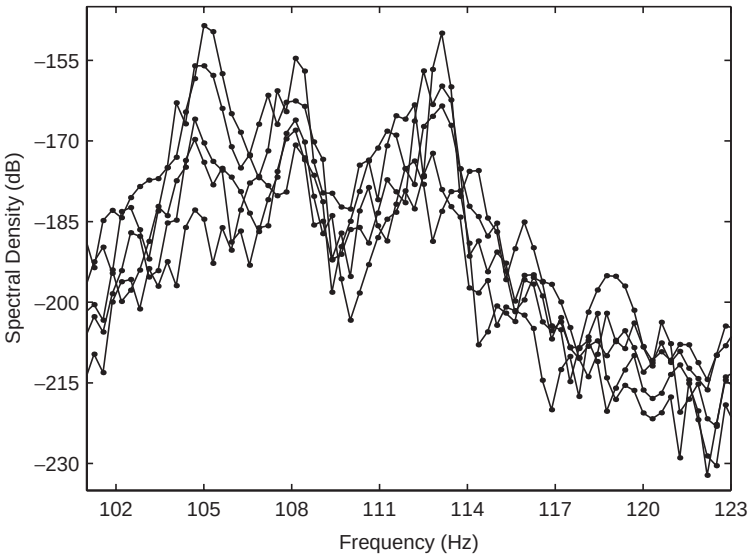

Fig. 7. Cross power spectra obtained without non-parametric rescaling: plate with ambient excitation, measurements 1–5. Bandwidth selection between 101 and 123 Hz.

as the result obtained by a single estimation on the 224 cross power spectra (no re-scaling taking into account). The effect of the non-stationary nature of the ambient excitation is clearly visible in the noisy mode shape estimates (shown for modes 2–3) obtained without taking the re-scaling into account (Figs. 6(a)–(b)). The fourth mode could not be identified with this approach due to the noisy character of the raw cross power spectral data (Fig. 7). On the other hand, the parametric approach was able to identify all 5 modes Table 2. Apart from the 224 cross power spectra, the same amount of auto power spectra (from the references) were taken into account for the estimation. Moreover, after the re-scaling procedure, the mode shape estimates are of relative good quality (Figs. 6(c)–(d)). The non-parametric procedure was also able to identify all 5 modes. The quality of the obtained mode shape estimates is superior to the results of the other methods (Figs. 6(e)–(f)). The reason for this can be found in the pre-scaling of the original cross power data before the estimation procedure. Fig. 8 compares the auto power spectral estimates of the first 5 reference measurements (in a frequency of 101–123 Hz) to the averaged auto power spectral estimates (dashed line) on a basis of all 224 references. The latter is of superior quality compared to the auto power spectra of any of the references separately. A comparison of Fig. 7 to Fig. 9 experimentally shows that by using the average of all 224 references (see Eq. (12)), pre-scaled data with a higher signal-to-noise ratio can be obtained than the original cross power spectra. The better the quality of the data, the better the estimation results.

3.2. *Civil engineering application: the Z24 bridge benchmark data*

Another example, where all intended d.o.f.'s are usually not be measured at the same time, is modal testing on civil structures. For further comparison and validation, both parametric and non-parametric mode shape reassembly approaches were tested on non-stationary ambient data obtained from a real civil engineering structure: the Z24 bridge benchmark data. Since both

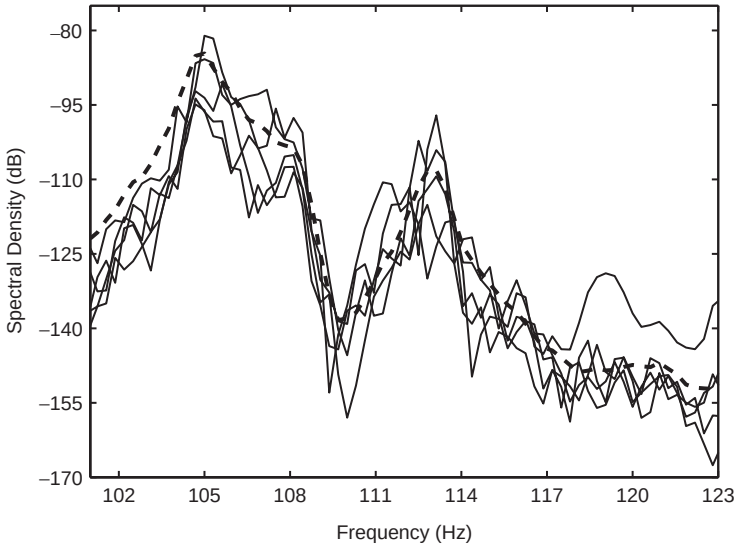

Fig. 8. Comparison of averaged (dashed line) and individual (full lines) auto power spectra: plate with ambient excitation, measurements 1–5. Bandwidth selection between 101 and 123 Hz.

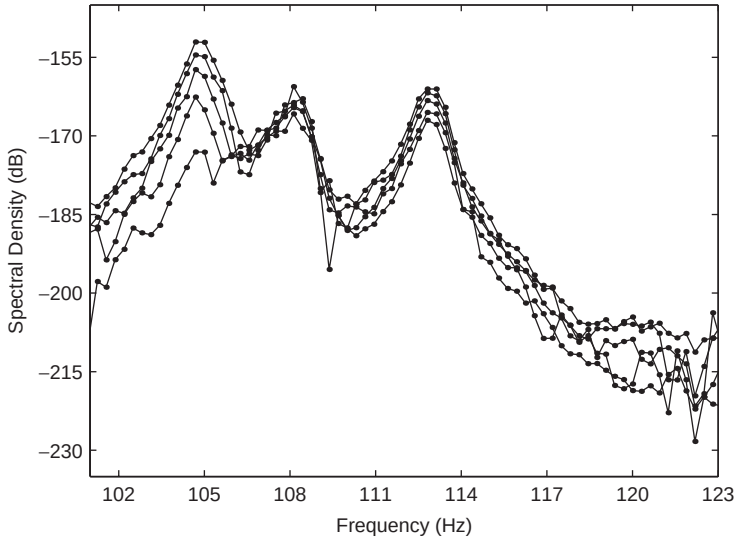

Fig. 9. Cross power spectra obtained with the non-parametric rescaling: plate with ambient excitation, measurements 1–5. Bandwidth selection between 101 and 123 Hz.

input–output and output-only modal testing were performed, the reassembled mode shape estimates from the ambient data can be easily validated on a basis of the results from the shaker data.

The Z24 bridge was an overpass of the national highway A1 between Bern and Zürich, Switzerland. It was a classical post-tensioned concrete box girder bridge with a main span of 30 m

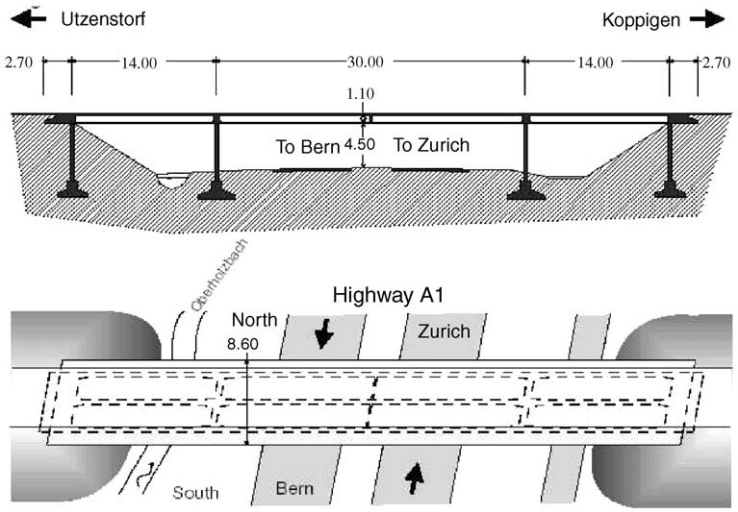

Fig. 10. Overview geometry of Z24 bridge.

and two side spans of 14 m (Fig. 10). Both abutments consisted of three concrete columns connected with concrete hinges to the girder. Both intermediate supports were concrete piers clamped into the girder. Part of the data assembled was made public as a civil engineering benchmark for comparing the performance of various system identification techniques [26]. The benchmark data consist of 9 patches with a total of 99 measurements including 3 reference measurements that were common to all patches. Data was sampled at 100 Hz while the anti-aliasing filter was set to 30 Hz. The ambient excitation sources on the bridge were wind, traffic on the highway and pedestrians part of the test crew. Each channel measured 65 536 samples, resulting in a measurement time of 10 min 55 s for each patch. For the input–output testing, two shakers were used. One was placed on a side span, the other at mid-span. The input signal was white noise between 3 and 30 Hz. The acquisition parameters were the same as during the ambient tests. More information about the bridge and the actual testing can be found in Ref. [27].

First of all, the raw time-domain data was transformed to the frequency domain. As mentioned in Ref. [16], a trade-off has to be made between obtaining a maximal number of averages in order to reduce stochastic errors and keeping an adequate block size (frequency resolution) in order to reduce leakage. The smaller the block size, the more leakage errors will be introduced into the measurements [28]. Moreover, the presence of the Hanning window will also have an increasing effect on the estimates. In order to make an adequate choice, several data sets containing H_1 FRF estimates, with block sizes ranging from 512 to 4096 time-domain samples, were considered. The estimation of modal parameters from these data sets, showed that the block size has an important effect on the damping ratio estimates. The damping ratios for the first 3 modes of the Z24 bridge, estimated on a basis of the H_1 data sets with varying block sizes, are shown in Fig. 11. It can be seen that the damping ratio estimates from the considered modes stabilize from about 2048 block size on. A block size of 4096 samples was eventually chosen for both input–output as well as output-only data sets. This choice of block size yields FRF and cross power estimates with 2048 spectral lines.

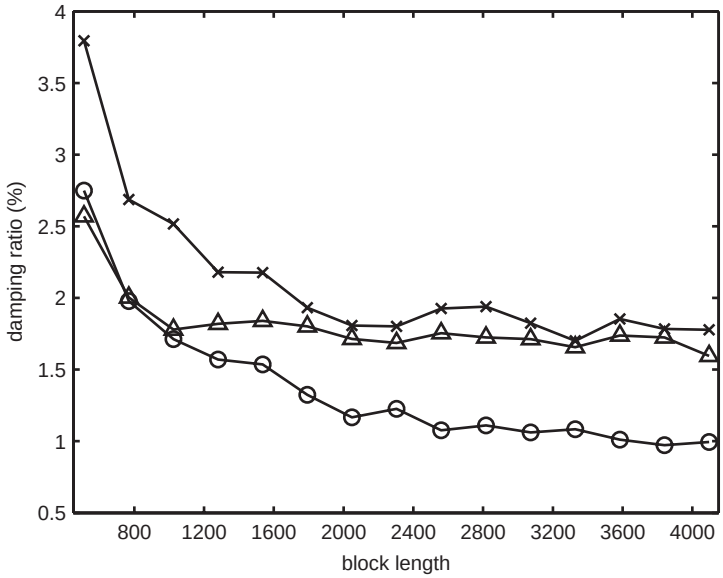

Fig. 11. Identified damping ratios from data sets with various block size: mode 1,'◦'; mode 2, '×'; mode 3, '△'.

Table 3
Overview of the estimation results obtained for the Z24 bridge

Mode	Shaker		Ambient			
	H_1		Parametric		Non-parametric	
	ω (Hz)	ξ (%)	ω (Hz)	ξ (%)	ω (Hz)	ξ (%)
1	3.87	0.91	3.86	0.65	3.86	0.74
2	4.83	1.69	4.90	1.56	4.90	1.65
3	9.78	1.53	9.76	1.24	9.78	1.27
4	10.52	1.57	10.24	1.15	10.23	1.91
5	12.42	3.10	—	—	12.47	5.56
6	13.28	4.56	—	—	—	—-
7	17.36	4.81	17.13	3.78	17.11	3.26
8	19.27	2.42	19.03	0.57	19.01	2.07
9	19.70	5.61	—	—	—	—-
10	26.67	3.28	26.71	3.17	26.60	3.26

On a basis of the FRF data (input–output shaker tests), a total of 10 modes were identified in the considered frequency band. An overview of the natural frequency and damping ratio estimates can be found in Table 3. An overview of the corresponding mode shape estimates can be found in Figs. 12 and 13. Although the bridge structure has a considerable amount of damping, all identified modes (apart from mode 7) were normal modes. The results are in good agreement with those obtained by other researchers and identification techniques, for instance those obtained with

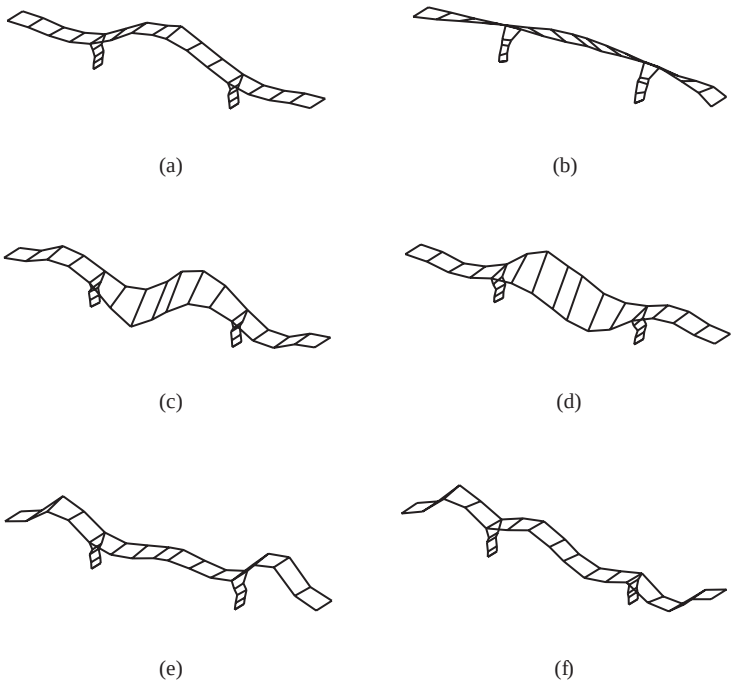

Fig. 12. Mode shape estimates obtained from the Z24 bridge with shaker excitation: modes 1–6, respectively indicated as a–f.

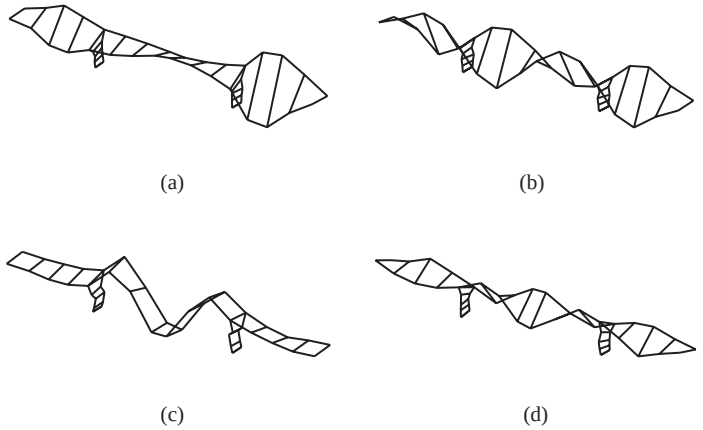

Fig. 13. Mode shape estimates obtained from the Z24 bridge with shaker excitation: modes 7–10, respectively indicated as a–d.

the subspace method [26]. Since FRFs are scaled quantities, no special re-scaling approaches were required for the correct assembly of mode shape estimates from the different patches.

For the ambient data set, the information of the references common to all patches is required for both the parametric and non-parametric mode shape re-scaling schemes in order to eliminate

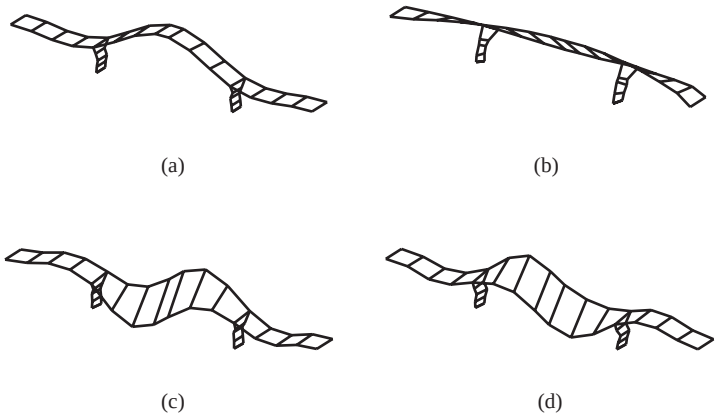

Fig. 14. Mode shape estimates obtained from the Z24 bridge with ambient excitation: modes 1–4, respectively indicated as a–d.

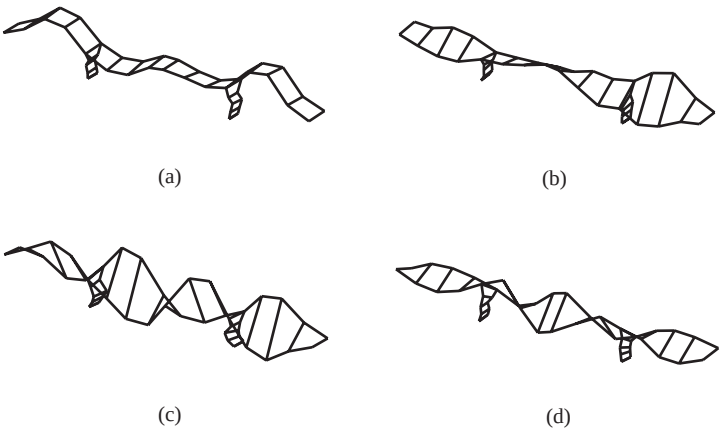

Fig. 15. Mode shape estimates obtained from the Z24 bridge with ambient excitation: modes 5, 7–8 and 10, respectively indicated as a–d.

the effect from the non-stationary excitation. An overview of the identified natural frequencies and damping ratios for both parametric and non-parametric approach, is given in Table 3. Due to the poor level of ambient excitation in the higher frequency range (11–30 Hz), not all modes could still be identified. The parametric approach was able to identify 7 out of 10 modes. The non-parametric approach added one more mode and stranded on 8 out of 10. A comparison between the results of shaker and ambient test shows that the differences in modal parameter estimates are generally small (Table 3). The discrepancies can be partly explained by temperature changes during the 1-day measurement period [26]. As shown in Ref. [29], temperature changes had a significant influence on the value of the eigenfrequencies of this bridge. The ambient mode shape estimates obtained with the non-parametric approach are shown in Figs. 14 and 15. A comparison between Figs. 12 and 13 and Figs. 14 and 15 shows a good agreement between the shaker and ambient test results. Similar results were obtained for the non-parametric approach. A more

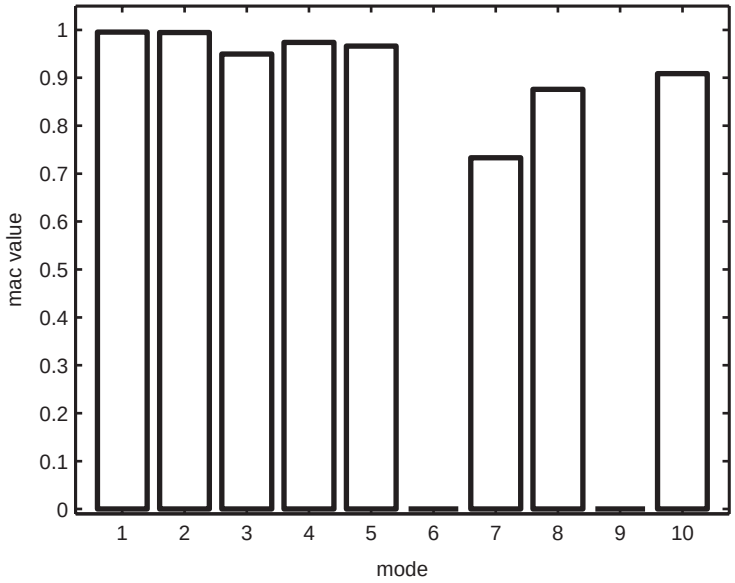

Fig. 16. Diagonal MAC values between corresponding mode shape estimates obtained with ambient and shaker excitation.

quantitative comparison, on a basis of MAC values between mode shape estimates obtained from ambient and shaker excitation, is shown in Fig. 16. Apart from mode 7, which was a highly complex mode, all MAC values are relatively high indicating a good agreement between the mode shapes found with both types of excitation.

4. Conclusions

In this contribution, two different approaches (a parametric and a non-parametric technique) were studied for correctly reassembling ('gluing' together) mode shape estimates from structures measured in different patches under non-stationary ambient excitation. The described techniques are able to compensate for the effect of both mode participation and excitation level non-stationarity. However, it is assumed that all data from the different patches contain information about the same system, i.e., data inconsistency is not taken into account.

Unlike the classic approach, where all patches are estimated separately, the results from the proposed techniques are based upon a single estimation procedure on the complete data set gathered by all patches. Apart from being less time consuming, both approaches have the advantage of yielding a single set of natural frequency and damping ratio estimates based on a larger amount of data. Moreover, the single estimation procedure eliminates the requirement for mode pairing the estimation results obtained from the separate analysis of patches.

For comparison and validation purposes, both approaches were tested on two cases were measurements are typically performed in patches: SLV experiments and in-operation civil engineering testing. A comparison of SLV-tests on a clamped composite plate and the Z24 bridge

benchmark data, showed a good agreement between the mode shape estimates (and other modal parameters) obtained from stationary (or input–output) and non-stationary ambient excitation. The non-parametric approach was found to produce results of slightly superior quality with respect to the other technique.

Acknowledgements

This research has been supported by the Fund for Scientific Research-Flanders (Belgium) (FWO), the Institute for the Promotion of Innovation by Science and Technology in Flanders (IWT) and by the Research Council (OZR) of the Vrije Universiteit Brussel (VUB).

References

[1] C. Krämer, C.A.M. de Smet, B. Peeters, Comparison of ambient and forced vibration testing of civil engineering structures, Proceedings of the 17th International Modal Analysis Conference (IMAC17), Orlando, FL, 1999, pp. 1030–1034.
[2] B. Peeters, G. De Rouck, Reference-based stochastic subspace identification for output-only modal analysis, Mechanical Systems and Signal Processing 13 (6) (1999) 855–878.
[3] P. Guillaume, L. Hermans, H. Van der Auweraer, Maximum likelihood identification of modal parameters from operational data, Proceedings of the 17th International Modal Analysis Conference (IMAC17), Orlando, FL, February 1999, pp. 1887–1893.
[4] L. Hermans, H. Van der Auweraer, Modal testing and analysis of structures under operational conditions: industrial applications, Mechanical Systems and Signal Processing 13 (2) (1999) 193–216.
[5] R.B. Randall, Y. Gao, J. Swevers, Updating modal models from response measurements, Proceedings of the 23rd International Conference on Noise and Vibration Engineering (ISMA23), Leuven, Belgium, 1998, pp. 1153–1160.
[6] O. Loland, J.C. Dodds, Experience in developing and operating integrity monitoring system in North Sea, Proceedings of the Eighth Annual Offshore Technology Conference, 1976, pp. 313–319.
[7] R. Nataraja, Structural integrity monitoring in real seas, Proceedings of the 15th Annual Offshore Technology Conference, 1983, pp. 221–228.
[8] T.R. Whittome, C.J. Dodds, Monitoring offshore structures by vibration techniques, Proceedings of Design in Offshore Structures Conference, 1983, pp. 93–100.
[9] C.Y. Kim, N.S. Kim, D.S. Jung, J.G. Yoon, Effect of vehicle mass on the measured dynamic characteristics of bridges from traffic-induced vibration test, Proceedings of the 19th International Modal Analysis Conference (IMAC19), Orlando, FL, 2001, pp. 1106–1111.
[10] S. Roberts, Identification of the modal parameters affecting automotive ride characteristics, Proceedings of the 19th International Modal Analysis Conference (IMAC19), Orlando, FL, 2001, pp. 270–274.
[11] E. Parloo, P. Verboven, P. Guillaume, M. Van Overmeire, Sensitivity-based operational mode shape normalization, Mechanical Systems and Signal Processing 16 (4) (2002) 659–675.
[12] H. Van der Auweraer, W. Leurs, P. Mas, L. Hermans, Modal parameter estimation from inconsistent data sets, Proceedings of the 18th International Modal Analysis Conference (IMAC18), San Antonio, TX, 2000, pp. 763–771.
[13] B. Cauberghe, P. Guillaume, B. Dierckx, Identification of modal parameters from inconsistent data, Proceedings of the 20th International Modal Analysis Conference (IMAC20), Los Angelos, CA, 2002.
[14] R.L. Mayes, S.E. Klenke, Consolidation of modal parameters from several exctration sets, Proceedings of the 19th International Modal Analysis Conference (IMAC19), Orlando, FL, 2001, pp. 1023–1028.
[15] L. Mevel, M. Basseville, A. Benveniste, M. Goursat, Merging sensor data from multiple measurement set-ups for non-stationary subspace-based modal analysis, Journal of Sound and Vibration 249 (4) (2002) 719–741.

[16] S. Marple, Lawrence Jr., Digital Spectral Analysis, Prentice-Hall, Englewood Cliffs, NJ, 1987.
[17] S.M. Kay, Modern Spectral Estimation: Theory and Application, Prentice-Hall, Englewood Cliffs, NJ, 1988.
[18] P.D. Welch, The use of fast fourier transform for the estimation of power spectra: a method based on time averaging over short modified periodograms, IEEE Transactions on Audio and Electracoustics AU-15 (1967) 70–73.
[19] W. Lisowski, Classification of vibration modes in operational modal analysis, Proceedings of the International Conference on Structural System Identification, Kassel, Germany, 2001, pp. 593–602.
[20] P. Guillaume, P. Verboven, S. Vanlanduit, Frequency-domain maximum likelihood estimation of modal parameters with confidence intervals, Proceedings of the 23rd International Seminar on Modal Analysis (ISMA23), Leuven, Belgium, September 1998, pp. 359–366.
[21] R. Pintelon, P. Guillaume, Y. Rolain, J. Schoukens, H. Van Hamme, Parametric identification of transfer function in the frequency domain—a survey, IEEE Transactions on Automatic Control 39 (11) (1994) 2245–2260.
[22] P. Guillaume, R. Pintelon, J. Schoukens, Robust parametric transfer function estimation using complex logarithmic frequency response data, IEEE Transactions on Automatic Control 40 (7) (1995) 1180–1190.
[23] J.S. Bendat, A.G. Piersol, Engineering Applications of Correlation and Spectral Analysis, Wiley, New York, 1980.
[24] P. Verboven, E. Parloo, P. Guillaume, M. Van Overmeire, Autonomous structural health monitoring—part 1: modal parameter estimation and tracking, Mechanical Systems and Signal Processing 16 (4) (2002) 637–657.
[25] R.J. Allemang, D.L. Brown, A correlation coefficient for modal vector analyis, Proceedings of the First International Modal Analysis Conference (IMAC1), Orlando, FL, 1982, pp. 110–116.
[26] B. Peeters, C.E. Ventura, Comparative study of modal analysis techniques for bridge dynamic characteristics, Mechanical Systems and Signal Processing, accepted for publication.
[27] C. Krämer, C.A.M. de Smet, G. De Roeck, Z24 bridge damage detection tests, Proceedings of the 17th International Modal Analysis Conference (IMAC17), Orlando, FL, 1999, pp. 1023–1029.
[28] P. Verboven, Frequency-domain System Identification for Modal Analysis, Ph.D. Thesis, Department of Mechanical Engineering, Vrije Universiteit Brussel, 2002.
[29] B. Peeters, G. De Roeck, One-year monitoring of the z24-bridge: environmental effects versus damage events, Eartquake Engineering and Structural Dynamics 30 (2) (2001) 149–171.